University of Bucharest - Faculty of Physics

Analysis algorithm for digital data used in nuclear spectroscopy

Bachelor Thesis

Răzvan LICĂ

Coordinators:
Dr. Nicolae Marius MĂRGINEAN, *IFIN-HH*
Dr. Mihaela SIN, *Faculty of Physics*

– 2012 –

Acknowledgments

This research project would not have been possible without the support and guidance of Dr. Nicolae Marius Mărginean. I am grateful for being included in the DFN-TANDEM group where I gathered valuable knowledge in nuclear spectroscopy.

I also wish to express my gratitude to all my professors from the Faculty of Physics, especially to Dr. Mihaela Sin who was very helpful and offered assistance and support in preparing my Bachelor Thesis.

Analysis algorithm for digital data used in nuclear spectroscopy

Abstract: Data obtained from digital acquisition systems used in nuclear spectroscopy experiments must be converted by a dedicated algorithm in order to extract the physical quantities of interest. I will report here the development of an algorithm capable to read digital data, discriminate between random and true signals and convert the results into a format readable by a special data analysis program package used to interpret nuclear spectra and to create coincident matrices.

The algorithm can be used in any nuclear spectroscopy experimental setup provided that digital acquisition modules are involved. In particular it was used to treat data obtained from the IS441 experiment at ISOLDE where the beta decay of ^{80}Zn was investigated as part of ultra-fast timing studies of neutron rich Zn nuclei. The results obtained for the half-lives of ^{80}Zn and ^{80}Ga were in very good agreement with previous measurements. This fact proved unquestionably that the conversion algorithm works. Another remarkable result was the improvement of ^{80}Ga level scheme but this makes the object of a future publication and will not be detailed here.

Keywords: data analysis algorithm, beta and gamma decay, isomeric level, nuclear lifetime, temporal clustering.

Contents

[1]The aspects presented in this appendix are summarised from a more complete description offered in [3]

Chapter 1

Introduction

1.1 Physical context

Many different historical models describe the atomic nucleus, none of which to this day completely explains experimental data on nuclear structure. The early models viewed the nucleus as a rotating liquid drop in which the long-range electromagnetic forces and relatively short-range nuclear forces cause behaviour which resembled surface tension forces in liquid drops of different sizes. It is successful at explaining many important phenomena of nuclei, such as their changing amounts of binding energy as their size and composition changes, but it does not explain the special stability which occurs when nuclei have special "magic numbers" of protons or neutrons. To explain the magic numbers there are proposed a number of models in which nucleons occupy orbitals, as shown in Fig. 1.1, much like the atomic orbitals in atomic physics theory.

These wave models imagine nucleons to be sizeless point particles in potential wells created by forces inside the nucleus (residual strong force and electromagnetic repulsion between the protons). This leads to energy quantization in a manner similar to the square well and harmonic oscillator potentials. In these models, the nucleons may occupy orbitals in pairs, due to being fermions, but the exact nature and capacity of nuclear shells differs from those of electrons in atomic orbitals.

There are however problems with theoretical models when an attempt is made to account for nuclear properties far away from closed shells. This represents an area of high interest for experimental physics, to investigate properties of exotic isotopes such as decay mechanisms, half-lives, energy of excited levels with spin and parity assignment and lifetimes for isomeric levels. The results obtained are compared with theoretical calculations and the final purpose is to improve the theoretical models and gain a better understanding of the subatomic universe.

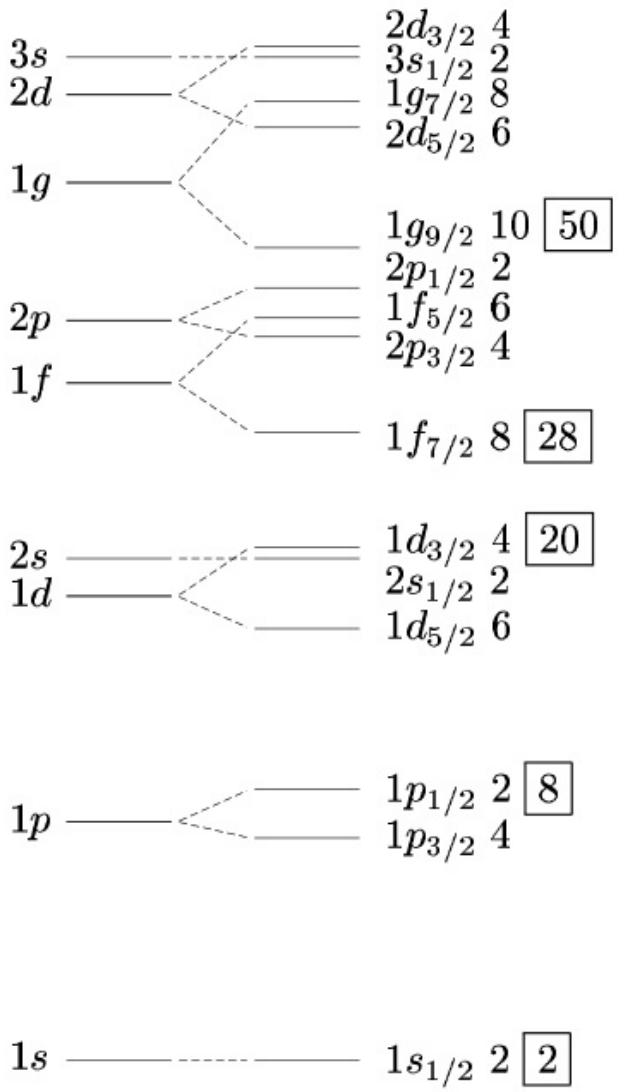

Figure 1.1: Low-lying energy levels in a single-particle shell model with an oscillator potential without spin-orbit (left) and with spin-orbit (right) interaction. The number to the right of a level indicates its degeneracy. The boxed integers indicate the magic numbers.

1.2 Motivation

Almost all the N = 49 isotones are known to have isomeric states with large spin differences compared to the ground states but in the case of ^{80}Ga no such state was discovered until recently. ^{80}Zn and the decay of ^{80}Zn to ^{80}Ga is of interest not only to nuclear structure physics but also to astrophysics for modelling the rapid process (*r-process*) in nucleosynthesis. The r-process takes place during a supernova explosion when neutron fluxes of 10^{32} $m^{-1}s^{-1}$ can be reached and the successive accumulation of many neutrons is much quicker than β or α decay processes. Elements heavier than lead can be produced in this process.

In 2010 a low-lying isomeric state in the exotic nucleus of ^{80}Ga was identified by collinear laser spectroscopy experiment [2]. The measurement was performed at ISOLDE, the *Isotope Separator On-Line facility* at CERN. Two hyperfine structures in ^{80}Ga were observed and one of them was the low-lying isomer with the half-life much greater than 200 ms. Both structures were assigned spins of I = 3 and I = 6. Shell model calculations suggested that the last one is the ground state.

Previous experimental investigations of ^{80}Zn decay reported in [6] did not include the newly found isomeric state. Complementary studies are required for determining the isomeric state and to measure properties such as the excitation energy and half-life.

1.3 What is required from an algorithm

In 2009 and 2011 at ISOLDE Ultra-Fast Timing measurements on heavy Ga nuclei at N = 50 and N = 49 were performed. Very interesting data was produced, but being recorded by digital modules it had to be further analysed in order to provide a physical interpretation for quantities such as life-times and for more elaborated energy level schemes to be obtained.

One of the main purposes of an algorithm was to convert the digital output obtained from Pixie4 digitizers into readable data for GASPware, a data analysis program package developed at Padova/Legnaro designed to treat data from GASP/EUROBALL.

Besides the data conversion, the algorithm is also required to differentiate between real physical events and background noise because, with digital

acquisition systems, all the signals are recorded and there is no hardware condition for removing the background. This should not be viewed as a drawback for digital systems, because recent technological advances permits us to store and operate huge amounts of data and with an intelligently crafted program one could obtain more physical information than compared to older analogic acquisition systems.

1.4 Overview of the ISOLDE facility

The On-Line Isotope Mass Separator ISOLDE is a facility dedicated to the production of a large variety of radioactive ion beams for many different experiments in the fields of nuclear and atomic physics, solid-state physics, materials science and life sciences. ISOLDE is one experimental infrastructure within the CERN complex of nuclear and particle physics experiments.

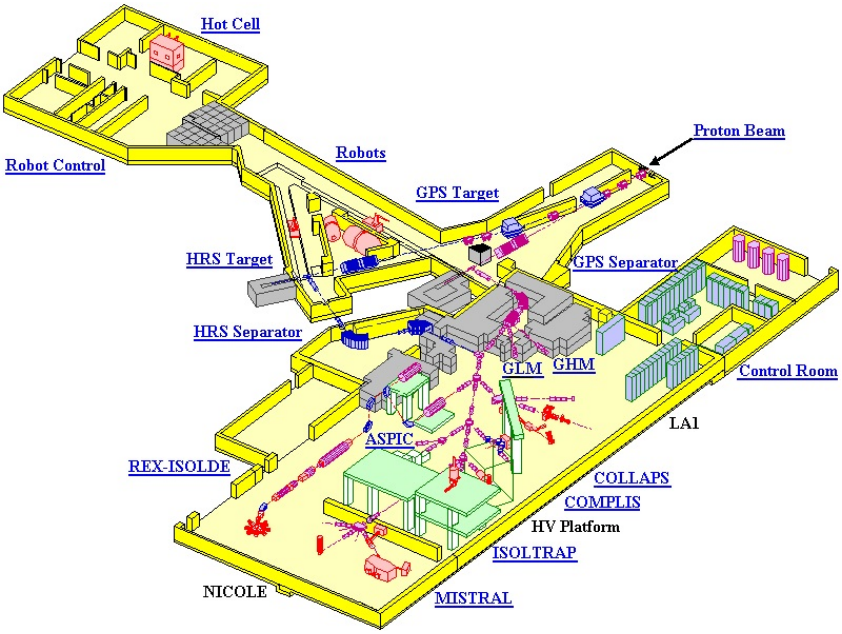

Figure 1.2: The ISOLDE facility is one of the world-leading laboratories for the production and investigation for radioactive nuclei.

The facility has been in operation since its start in 1967 and is presently receiving protons from the Proton Synchrotron Booster (PSB) of CERN. The success of ISOLDE is due to the continuous development of new radioactive ion beams and improvement of the experimental conditions. With the up-

coming high energy and intensity upgrade HIE-ISOLDE, the possibilities for experiments with exotic nuclei will be further boosted.

The member states of the ISOLDE Collaboration are Belgium, Denmark, Finland, France, Germany, Greece, Ireland, Italy, Norway, Romania, Spain, Sweden and the United Kingdom.[1]

The experiments at ISOLDE focus mainly on modern nuclear structure physics. In addition, front-line studies in other fields are pursued. The energy range of the investigated radionuclides goes from 10^{-6} eV in the case of low-temperature nuclear orientation at NICOLE to 3 MeV per nucleon in the case of post-accelerated beams at REX-ISOLDE.

Another closely related field of research is nuclear astrophysics. Nuclear masses and half-lives of exotic nuclides need to be known in order to calculate nucleosynthesis processes. In addition, decay properties including beta-delayed particle emission have to be understood in order to consider them in the theoretical models. Low-energy reaction cross-sections provide valuable input for the understanding of the various processes in stars. ISOLDE also hosts experiments that investigate fundamental interactions. Especially Penning trap experiments are dedicated to fundamental tests since they are able to provide very precise data that are needed to further push the limits for new physics beyond the Standard Model.

[1] Based on data from Dec. 2010 provided in [1]

Chapter 2

The *pixie2gasp* algorithm

2.1 Overview

The program was written in the C programming language under a Linux distribution. Its development and testing phase required almost two months of work. One of the very important achievements was the short execution duration of the program. In Table 2.1 was printed the output of analysing one *.bin* file with raw data from the *IS441/2011* experiment.

Table 2.1: The command-line output for *pixie2gasp*

Command-line output	Description
./p2g.out 80Ga_list_0080.bin	p2g.out represents the executable and requires as argument the name of the file to be compiled
Events in file 1 : 31614818	The number of signals recorded in the .bin file
Time elapsed: 6.840000	Time elapsed reading the input
quickSort: 12.950000	Time elapsed sorting the data: $12.95 - 6.84 = 6.11 seconds$
TrueEvents in file 1: 5020894	Number of true events (clusters) identified by temporal clustering algorithm
Time elapsed: 17.360000	Time elapsed to identify the clusters: $17.36 - 12.95 = 4.41 seconds$
TotalTime: 21.690000	Time elapsed writing to disk the new .bin file converted in GASPware format: $21.69 - 17.36 = 4.33 seconds$

Even if the program is functional and provides very good results, there are still some improvements scheduled for future development such as minimizing

memory use, merging the main program and the sub-programs to compile into a single executable and implementing the possibility for the user to provide the various parameters in a configuration ASCII file rather than predefining the parameters of an experimental set-up inside the code.

The program has four main parts consisting of reading and applying corrections to the input data, implementing a sorting algorithm, applying a temporal clustering algorithm and finally exporting the data into the desired format. In the following sections I will present each aspect concerning these four main parts shown in Fig. 2.1.

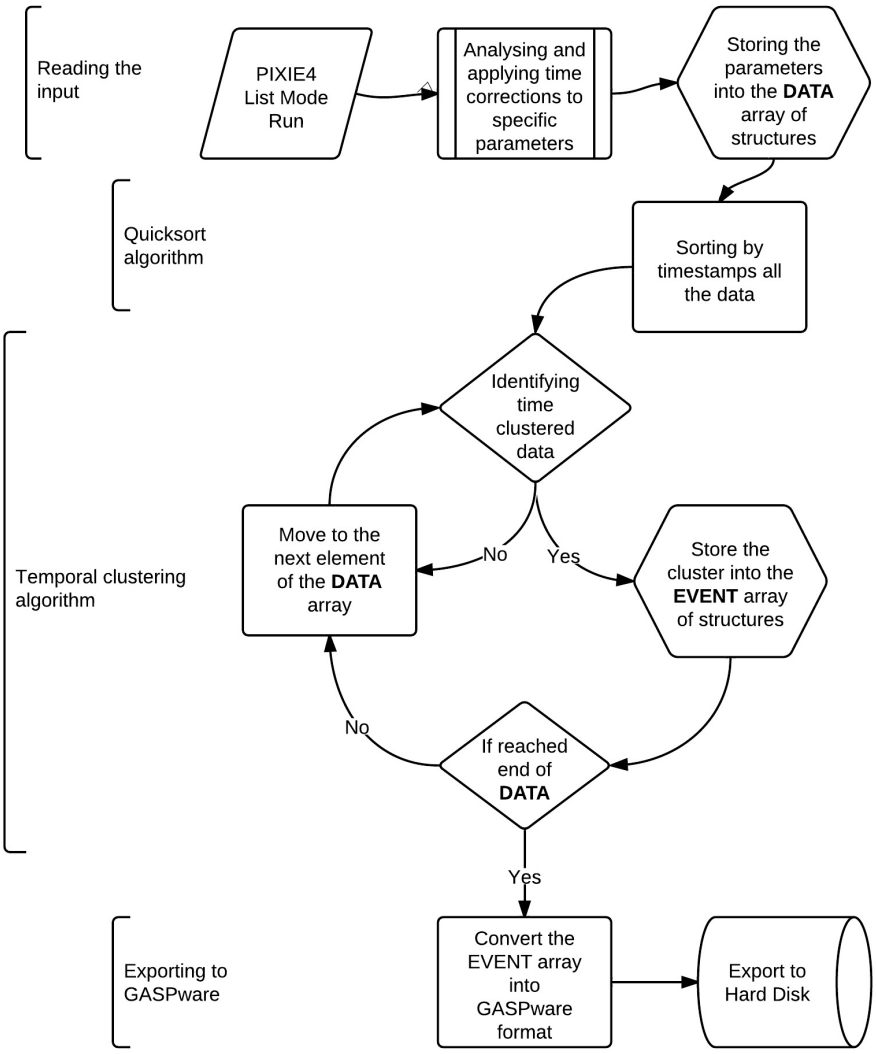

Figure 2.1: The *pixie2gasp* algorithm flowchart.

2.2 Reading the input

2.2.1 The DGF-Pixie4 output

The Digital Gamma Finder (DGF) [4] family of digital pulse processors features unique capabilities for measuring both the amplitude and shape of pulses in nuclear spectroscopy applications. The DGF architecture was originally developed for use with arrays of multi-segmented HPGe gamma-ray detectors, but has since been applied to an ever broadening range of applications.

The DGF Pixie-4 is a 4-channel all-digital waveform acquisition and spectrometer card based on the CompactPCI/PXI standard for fast data readout to the host. It combines spectroscopy with waveform capture and on-line pulse shape analysis. The Pixie-4 accepts signals from virtually any radiation detector. Waveforms, timestamps, and the results of the pulse shape analysis can be read out by the host system for further off-line processing.

The output of the DFG-Pixie4 modules represents the input for *pixie2gasp*. The DGF modules provide a list mode run which acquire data on an event-by event basis. The output data of list mode runs can be reduced by using one of the compressed formats described in the User's Manual.

The list mode data in external memory consists of 32 local I/O data buffers. The local I/O data buffer can be written in a number of formats. The buffer content always starts with a buffer header of length BUFHEADLEN. Currently, BUFHEADLEN is six, and the six words are listed in the next table.

Table 2.2: *Buffer header data format*

Word#	Variable	Description
0	NDATA	Number of words in this buffer
1	MODNUM	Module Number
2	FORMAT	Format descriptor = RunTask +0x2000
3	TIMEHI	Run start time, high word
4	TIMEMI	Run start time, middle word
5	TIMELO	Run start time, low word

Following the buffer header, the events are stored in sequential order. Each event starts out with an event header of length EVENTHEADLEN. Currently, EVENTHEADLEN=3, and the three words are:

Table 2.3: *Event header data format*

Word#	Variable	Description
0	PATTERN	Hit pattern
1	TIMEHI	Event time, high word
2	TIMELO	Event time, low word

The hit pattern is a bit mask, which tells which channels were read out plus some additional status information. For example if channels 1 and 4 were hit, the hit pattern will be 1001, and if channels 1, 2, 3 were hit, it will be 1110.

The data for each channel are organized into a channel header of length CHANHEADLEN, which may be followed by waveform data. CHANHEADLEN depends on the run type and on the method of data buffering. In the case of the 2009 and 2011 experiment, compression 3 List Mode (RUNTASK = 259) was used, with CHANHEADLEN=2, and the two words being

Table 2.4: *Channel header data format*

Word#	Variable	Description
0	TRIGTIME	Fast trigger time
1	ENERGY	Energy

2.2.2 Reading the time-stamp for each pulse

Pixie-4 records time information in three different locations: the buffer header, the event header and the channel header. In the Pixie-4, there is a 48-bit time counter that is reset to zero at boot time or at a run start with the 'synchronize clocks' option selected. It is incremented at the full processor

clock rate of $75MHz$ so the unit time is $13.33ns$. Hence, the 48-bit word can span a time interval of 43.44 days before rolling over. At the beginning of a data acquisition run, the module looks at the counter and records the BufferTime as a 48-bit number, using three 16-bit words. These three words are the time stamps in the buffer header (BUF_TIMEHI, BUF_TIMEMI, BUF_TIMELO). Every time an event is recognized, the the lower 32-bit of the time counter are recorded as two 16-bit words in the event header (EVT_TIMEHI, EVT_TIMELO). Every time a channel triggers at the rising edge of a pulse, the channel records the lowest 16 bit of the time counter, which is reported in the channel header (CHAN_TRIGTIME). As the rising edge occurs a filter time before the event is recognized, the channel time is typically a few microseconds ahead of the event time. In conclusion, to obtain the most precise time stamp for a pulse, the program should record the time as a 48-bit number with the HI part (BUF_TIMEHI) MI part (EVT_TIMEHI) and LO part (CHAN_TRIGTIME) and consider the overflow of the MID and LO 16-bit words.

The overflow correction can be done in two ways: by increasing the first digit of the higher word when the current word has overflowed, or by increasing the values stored in neighbouring addresses of memory by the values stored in HI, MI, LO.

```
ch->time = buffer->timehi;
ch->time <<= 16;
ch->time += event->timehi;
ch->time <<= 16;
ch->time += channel->trigtime;
```

2.2.3 Time correlation for the timestamps

A very important step in analyzing the input is applying time corrections to each input signal so that it will compensate the delays that could appear due to the electronic connections or the digital analysis for the pulses. This can be done with a modified version of the main *pixie2gasp* program which only builds a histogram of the time differences between two desired channels. The user can calculate the time difference between them provided that the signals were coincident.

In the current set-up, all the detectors should record coincident signals because the physical processes involved were mostly beta decay followed by

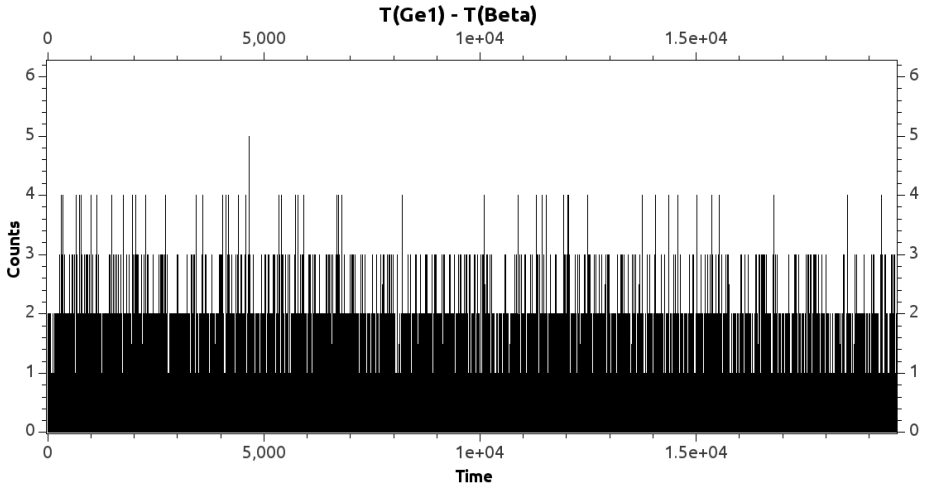

Figure 2.2: Time difference between two uncorrelated signals. Calculating the time difference $t_{ge1} - t_{beta}$ between a Beta signal and the first following HPGe signal will provide random results for different signals.

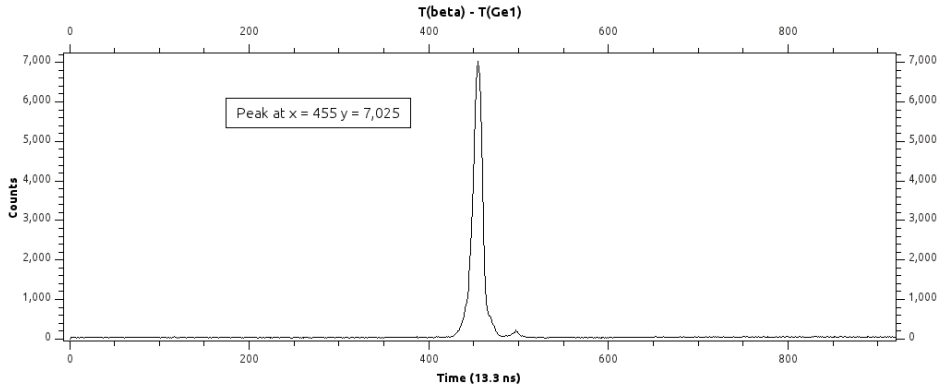

Figure 2.3: Time difference between two detectors in correlation. The time difference between a HPGe and the immediately following Beta signal is $t_{beta} - t_{ge1} = 455 \cdot 13.3ns = 6.05\mu s$. The signal from HPGe1 comes earlier than the signal from the beta sillicon detector and the difference is constant because it is caused only by electronic connections.

the gamma dezexcitation of the nucleus that are almost spontaneous (the lifetimes of the excited states are of three orders of magnitude lower than the 13.3ns unit time). Based on this fact, for each detector a corresponding correction related to a reference detector (e.g. the beta detector) should be applied.

2.3 Sorting algorithm

When the data buffers are full, they are written on the disk in their completion order, so that the chronological order of the recorder events is not maintained. To continue with the analysis, the data must be sorted by the corrected timestamps. The most important requirement for a sorting algorithm was the time of execution which is directly proportional with the number of steps taken to sort a certain number of data. In the following table, there are some popular sorting algorithms.

Table 2.5: *Comparison of sorting algorithms*

Name	Best	Average	Worst	Memory	Method
Quicksort	$n \cdot log(n)$	$n \cdot log(n)$	n^2	$log(n)$	Partitioning
Mergesort	$n \cdot log(n)$	$n \cdot log(n)$	$n \cdot log(n)$	n	Merging
Bubblesort	n	n^2	n^2	1	Exchanging
Binary tree sort	n	$n \cdot log(n)$	$n \cdot log(n)$	n	Insertion

A quadratic behaviour was unwanted because of the amount of time required to sort a list. The best behaviour was $O(nlog(n))$ and *quicksort* was the most stable and memory efficient solution. In the worst case, it makes n^2 comparisons, though this behavior is encountered only in very specific distributions of the data. It is often faster in practice than other $O(nlog(n))$ algorithms.

Quicksort is a divide and conquer algorithm. It first divides a large list into two smaller sub-lists: the low elements and the high elements and then recursively sorts the sub-lists. The *quicksort* code displayed below was used in *pixie2gasp* to sort a structure array that contained all the raw data from one *.bin* file.

```
void quickSort(struct date *arr, int left, int right){
      int i = left, j = right;
      struct date tmp;
      u_int64_t pivot = arr[(left + right)/2].time;

      /* partition */
      while (i <= j) {
            while (arr[i].time < pivot)
                  i++;
            while (arr[j].time > pivot)
                  j--;
            if (i <= j) {
                  tmp = arr[i];
                  arr[i] = arr[j];
                  arr[j] = tmp;
                  i++;
                  j--;
            }
      };

      /* recursion */
      if (left < j)
            quickSort(arr, left, j);
      if (i < right)
            quickSort(arr, i, right);
}
```

The steps are:

1. Pick an element, called a pivot, from the list.

2. Reorder the list so that all elements with values less than the pivot come before the pivot, while all elements with values greater than the pivot come after it (equal values can go either way). After this partitioning, the pivot is in its final position. This is called the partition operation.

3. Recursively sort the sub-list of lesser elements and the sub-list of greater elements.

2.4 Temporal Clustering

2.4.1 Definition of a cluster

A cluster is represented by two or more signals that come one after another inside a specific time interval or *gate*. The signals are called *prompt*, and can be considered as coming from the same decaying nucleus. The time interval is usually hundreds of nanoseconds which is one order of magnitude higher than the time resolution of the slowest detectors, the high purity germanium.

After the data is sorted, if the correlation of detectors was precise, the temporal distribution of the signals should be clustered around the moments when nuclear decay occurred. The nuclear decay will be triggered by the production of isotopes when a proton pulse hits the uranium target. In Figure 2.4 was represented schematically the clustered distribution of signals.

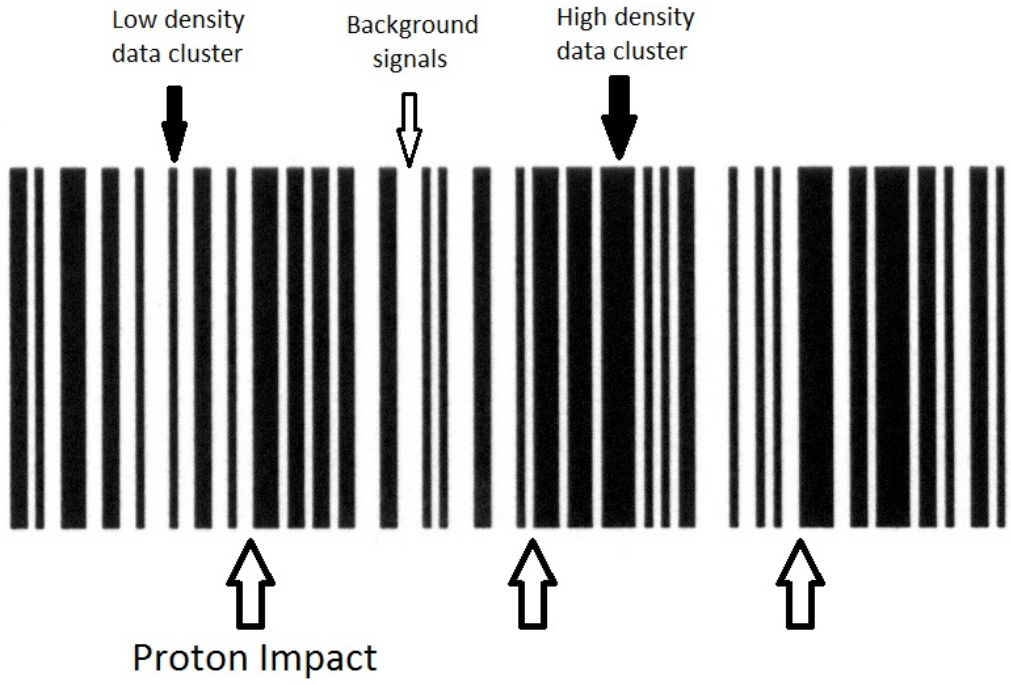

Figure 2.4: The density of clusters becomes smaller as time passes from the last proton pulse.

2.4.2 Background reduction

It is very important to distinguish between random events, called the background, and real events. By a very high probability inside a cluster we will have only real events and no background. Figure 2.5 shows the the spectra recorded with a HPGe detector without background reduction.

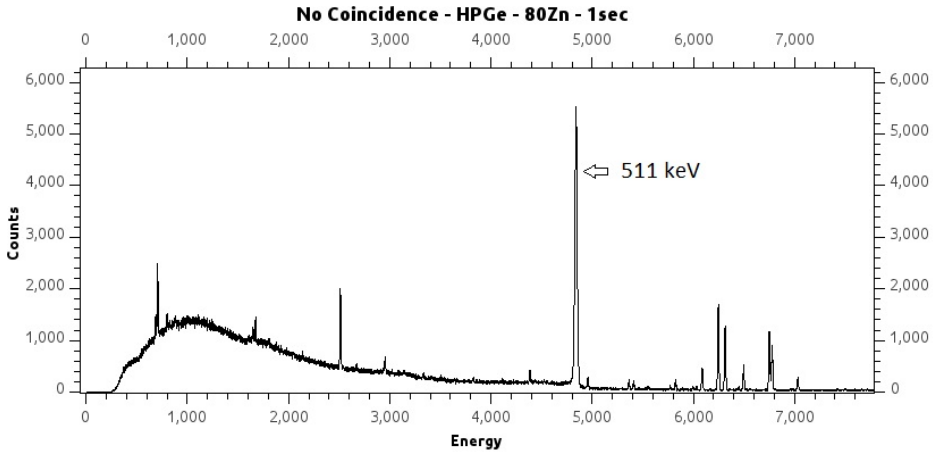

Figure 2.5: HPGe spectra with no temporal clustering.

The $511keV$ photons are produced by pair annihilation of positrons and electrons in the entire chamber volume. Neutrons are activating various stable elements which decay by gamma emission, and some high energy gamma rays produce positron-electron pairs by the well known pair production mechanism. These reactions are not related to the beta decaying isotopes of interest, so the detectors record this annihilation photons as background radiation. By using the clustering technique, we can observe in Figure 2.6 how the $511keV$ peak reduces along with the background.

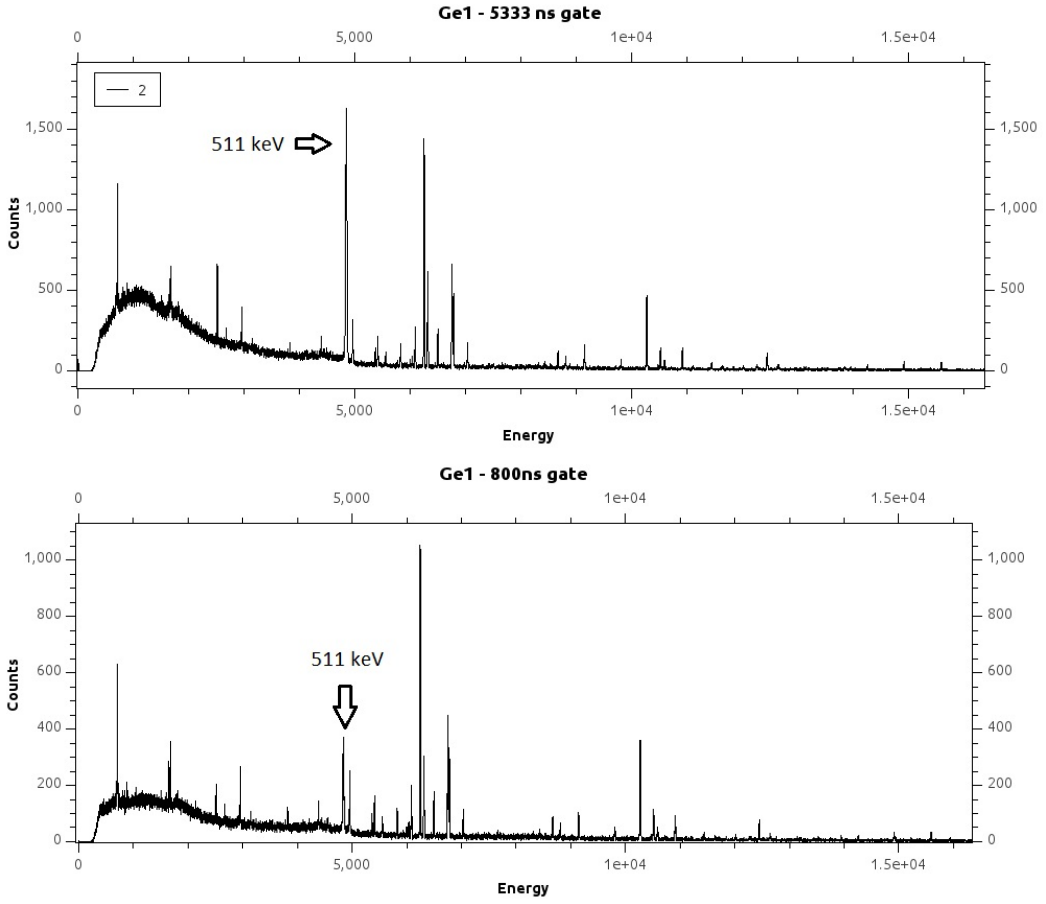

Figure 2.6: HPGe spectra with temporal clustering using a gate of $5.3ms$ and $800ns$. The background reduction can be observed by the reduction of the annihilation peak. Using a smaller gate, the reduction is more intense.

2.5 Parameters of interest. Output

Each cluster represents a group of at least two coincident signals. For each signal the following parameters of interest are recorded:

1. Energy value – the amplitude recorded by the corresponding detector.
2. Low-resolution time – relative to the precedent proton pulse. It is of very high interest for beta decay lifetime measurement. The unit time is 10 ms.
3. High-resolution time – represents the exact moment of time when a signal was recorded inside the cluster, as shown in Fig. 2.9. The unit time is 13.3 ns. This parameter is used for gating the prompt signals. The high resolution time is defined by the formula:

$$t_{hr(i)} = \frac{1}{n}\sum_{i=1}^{n} t_i - t_i + c$$

   t_i – exact timestamp of a signal relative to the proton pulse and has the unit of $13.3ns$.
   n – total number of signals in the cluster.
   c – offset.

4. TAC amplitude (only if present) – provided by a Time to Amplitude Converter and is used for ultra-fast timing measurements of picosecond order.

Each cluster contained several auxiliary parameters such as:

1. Event size – number of signals in each cluster
2. Proton intervals (2 parameters) – time intervals between the last two proton pulses and between the current and next proton pulse. This was used because, as shown in Fig.2.7 , the proton pulses were not coming at the same time intervals, but at multiples of 1.2 seconds. This produced the stair-like shape of the low resolution time for gamma signals as seen in Fig. 2.8 .

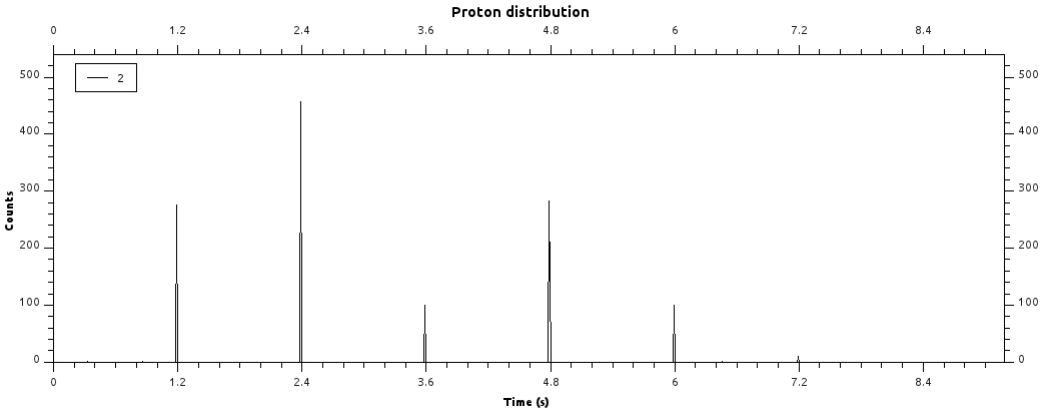

Figure 2.7: Distribution of intervals between proton pulses.

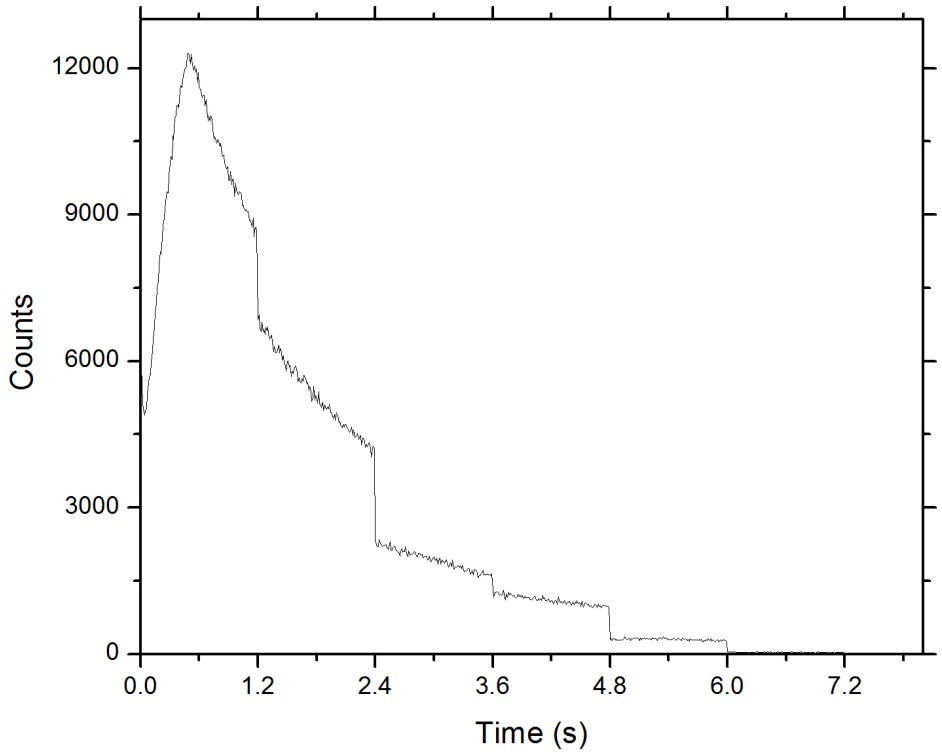

Figure 2.8: Low resolution time spectra for gamma signals when no condition is used on gating the proton intervals.

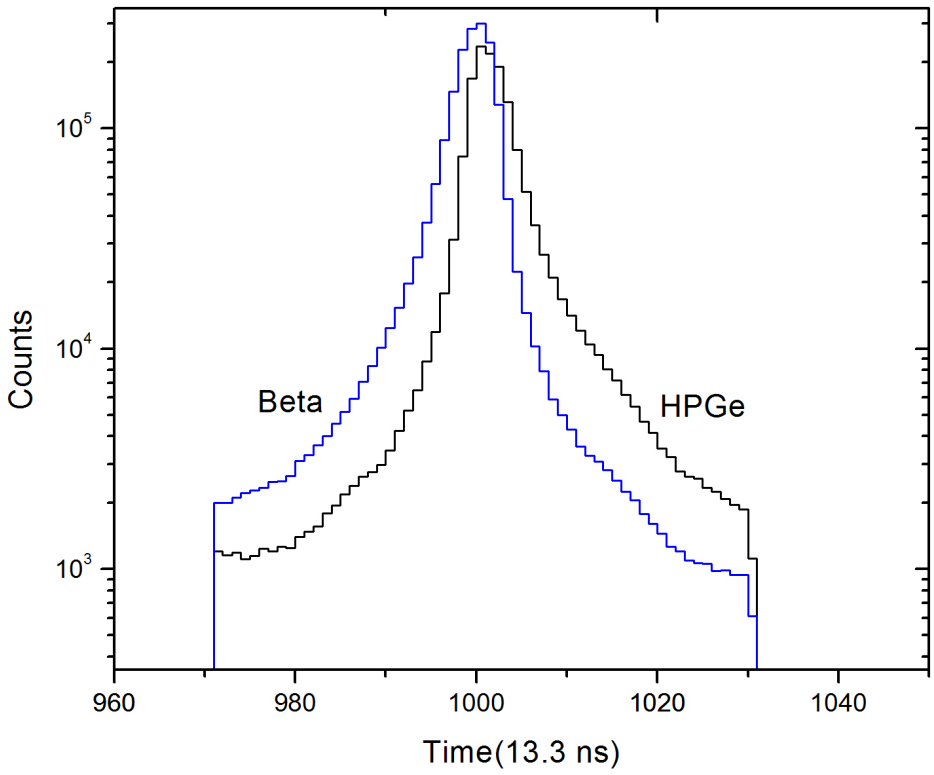

Figure 2.9: High resolution time spectra for gamma and beta signals.

Chapter 3

Results

3.1 Half-life measurement for ^{80}Zn and ^{80}Ga

3.1.1 Data analysis

To perform the half-life measurement for ^{80}Zn and ^{80}Ga a 2D matrix was created. This matrix contained the low resolution time values on one axis and energy values on the other axis for the signals coming from the HPGe detectors. Additional background reduction was possible by gating the prompt beta and gamma signals.

The current experiment required another condition regarding the proton intervals. The best configuration would be to gate a long current proton interval. This is because no other proton pulse should produce decaying isotopes during the decay of the last implanted isotopes.

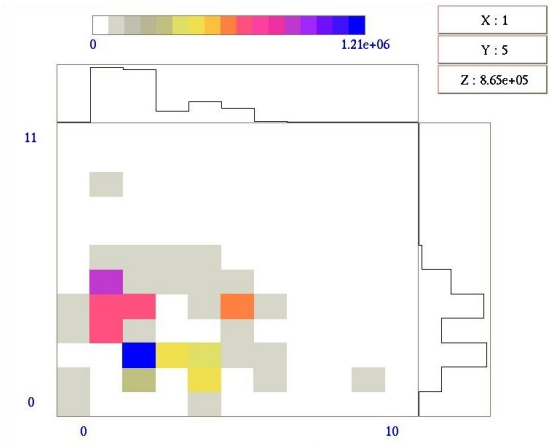

Figure 3.1: Distribution of signals depending on "previous" and "current" proton intervals. On X axis are shown the "previous" intervals and on Y axis the "current" intervals.

As shown in Fig. 3.1, a great fraction of the signals were produced when the previous proton interval had value 1 (1.2 seconds) and the current proton interval had value 5 (6 seconds). Intervals 1-5 were used as gating conditions.

After applying the earlier mentioned conditions through GASPware analysis software package, the time-energy matrix shown in Fig. 3.2 was obtained. Note that there is no more a stair-like appearance of time spectra, as a result of gating the proton intervals. The colours represent the number of signals arriving in the specific time and energy channel. The long horizontal intense lines indicate γ transitions of the long lived (^{80}Ge, ^{80}As) or stable (^{80}Se) isobars in the A=80 decay chain.

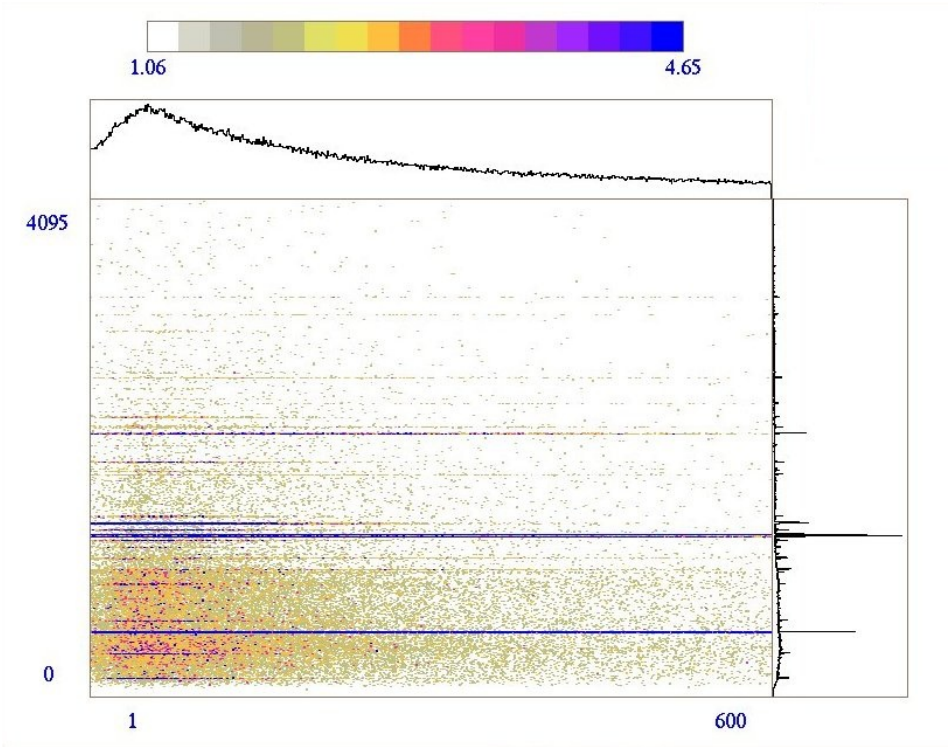

Figure 3.2: Time-Energy 2D matrix of HPGe signals. representing the distribution of signals depending on their time of detection (X axis) and energy (Y axis).

By investigating the time distribution of gamma transitions from the daughter nuclei, the parent's half-life can be found. In Table 3.1 are listed the most intense gamma transitions which were taken into account for the current analysis. In Fig. 3.4 is represented the energy gated time spectra and the half-lives calculated according to Appendix A, Section A.1. λ is directly

computed by taking the linear fit of the semi-logarithmic representation of the decay region.

$$ln(N/N_0) = -\lambda t$$

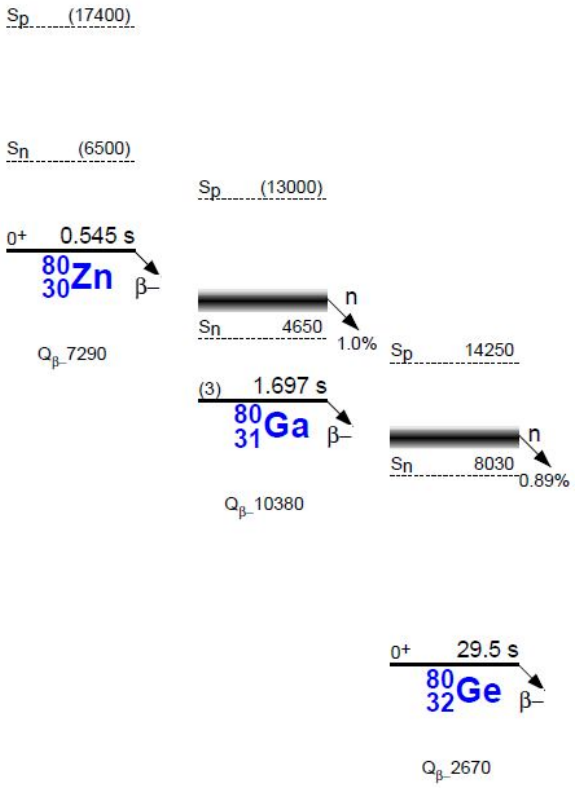

Figure 3.3: The decay chain of mass A=80 isotopes of interest. Figure taken from Table of Isotopes, Eighth Edition, 1999 Update.

Table 3.1: *Most intense transitions from ^{80}Ga and ^{80}Ge.* Data taken from ENSDF

^{80}Ga		^{80}Ge	
E_γ keV	I_γ %	E_γ keV	I_γ %
642.21 *5*	32.0 *21*	659.14 *4*	100 *3*
685.60 *5*	34.0 *21*	1083.47 *4*	62 *2*
712.53 *5*	100 *5*	1109.36 *4*	23.8 *8*
715.40 *5*	75 *4*		

3.1.2 Results and conclusions

The computed values for the lifetimes extracted from IS441/2009 data are in very good agreement with existing results. In Table 3.2 are listed the values taken from ENSDF. Note that the precision of evaluating the half-life of ^{80}Zn in the current experiment is improved comparing to previous values. A 4 seconds interval was more than enough to gather statistics for ^{80}Zn. In the case of ^{80}Ga the maximum available interval of 6 seconds is not providing sufficient statistics to obtain an improvement in precision.

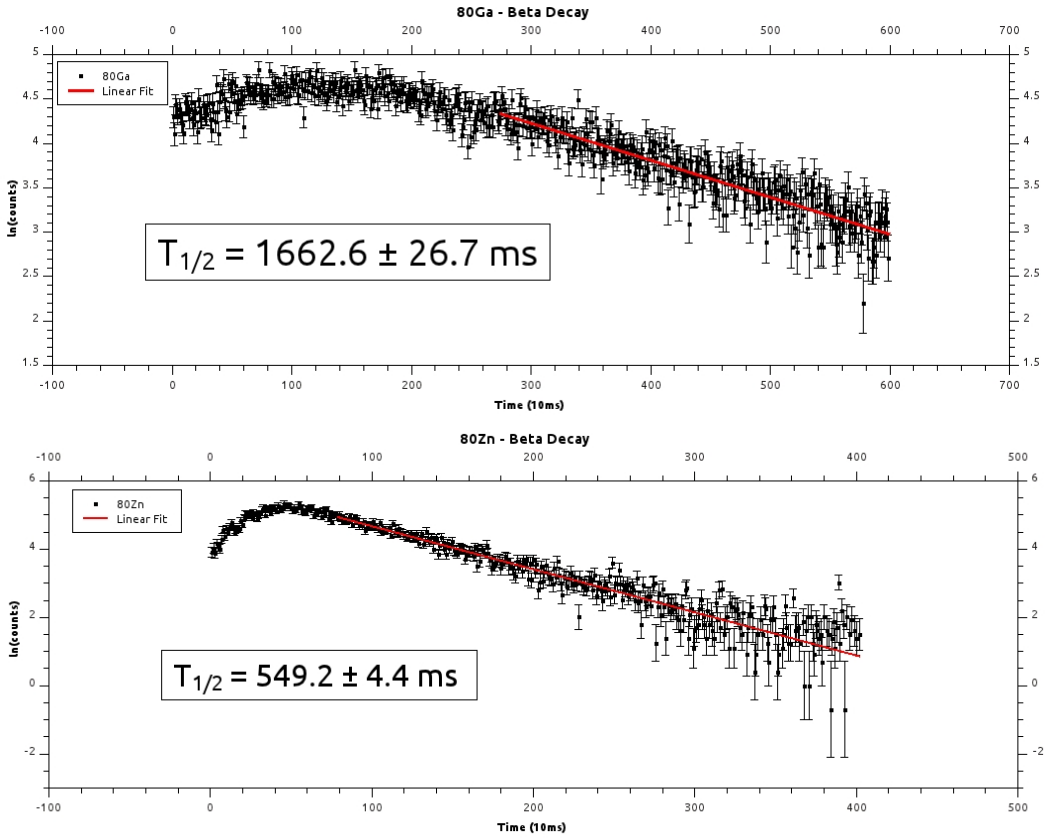

Figure 3.4: Semi-logarithmic representation of the activation and decay for ^{80}Zn and ^{80}Ga.

Table 3.2: *Comparison between current and previous half-life measurements*

	$T_{1/2}$[a]	Previous $T_{1/2}$[a]
^{80}Zn	0.549 s 4	0.54 s 2[b]
^{80}Ga	1.662 s 27	1.676 s 14[c]

[a] the second number represents the precision of the last digits.
[b] weighted average of 0.54 s 3 (1991Kr15), 0.55 s 2 (1986Gi07) and 0.53 s 5 (1986Ek01)
[c] weighted average of 1.65 s 1 (1993Ru01), 1.706 s 10 (1991Kr15), 1.67 s 10 (1982FoZZ), 1.66 s 2 (1976Ru01) and 1.7 s 2 (1974Gr29)

Appendix A

Brief theoretical aspects

A.1 The radioactive decay law[1]

Radioactivity represents changes in the individual atoms and not a change in the sample as a whole. The decay is statistical in nature, it is impossible to predict when any given atom will disintegrate and this hypothesis leads directly to the *exponential law*. The lack of predictability of the behaviour of single particles is understood in the context of quantum theory.

If N radioactive nuclei are present at time t and if no new nuclei are introduced into the sample, then the number dN decaying in a time interval dt is proportional to N, and so

$$\lambda = -\frac{dN/dt}{N}$$

in which λ is a constant called the *disintegration (or decay) constant*. The right side of the equation is the probability per unit time for the decay of an atom. That this probability is constant, regardless of the age of the atoms, is the basic assumption of the statistical theory of radioactive decay. Integrating the previous equation leads to the *exponential law of radioactive decay*

$$N(t) = N_0 e^{-\lambda t}$$

where N_0, the constant of integration, gives the original number of nuclei present at $t = 0$. The half-life $t_{1/2}$ gives the time necessary for half of the nuclei to decay. Putting $N = N_0/2$ in the above equation gives

$$t_{1/2} = \frac{ln(2)}{\lambda}$$

[1]The aspects presented in this appendix are summarised from a more complete description offered in [3]

A.2 Theory of β decay

The nucleus can correct a proton or a neutron excess by directly converting a proton into a neutron or a neutron into a proton. This process can occur in three possible ways, each of which must involve another charged particle to conserve electric charge (the charged particle, originally called a β particle, was later shown to be identical to ordinary electrons).

$$\begin{aligned} \mathrm{n} &\rightarrow \mathrm{p} + \mathrm{e}^- + \bar{\nu} \qquad \beta^- \text{ decay} \\ \mathrm{p} &\rightarrow \mathrm{n} + \mathrm{e}^+ + \nu \qquad \beta^+ \text{ decay} \\ \mathrm{p} + \mathrm{e}^- &\rightarrow \mathrm{n} + \nu \qquad \text{electron capture } (\varepsilon) \end{aligned}$$

The first process is knows as negative β decay or negatron decay and involves the creation and emission of an ordinary electron. The second process is positive β decay or positron decay, in which a positively charged electron is emitted. In the third process, an atomic electron that strays too close to the nucleus is swallowed, allowing the conversion of a proton to a neutron.

In all three processes, another particle called a *neutrino* is also emitted, but since the neutrino has no electric charge, its inclusion in the decay process does not affect the identity of the other final particles.

In a nucleus, β decay changes hoth Z and N by one unit: $\mathrm{Z} \rightarrow \mathrm{Z} \pm 1$, $\mathrm{N} \rightarrow \mathrm{N} \mp 1$ so that $\mathrm{A} = \mathrm{Z} + \mathrm{N}$ remains constant. Thus β decay provides a convenient way for an unstable nucleus to "slide down" the mass parabola as shown in Fig. 3.3 of constant A and to approach the stable isobar.

A.3 Theory of γ decay

Radioactive γ emission is analogous to the emission of atomic radiations such as optical or X-ray transitions. An excited state decays to a lower excited state or possibly the ground state by the emission of a photon of γ radiation of energy equal to the difference in energy between the nuclear states (less a usually negligible correction for the "recoil" energy of the emitting nucleus). Gamma rays have energies typically in the range of 0.1 to 10 MeV and their emission is observed in all nuclei that have excited bound states (A>5). It usually follows α and β decays since those decays will often lead to excited states in the daughter nucleus.

The half-lives for γ emission are usually quite short, generally less than 10^{-9} s, but occasionally we find half-lives for γ emission that are significantly longer, even hours or days. These transitions are known as *isomeric transitions* and the long-lived excited states are called *isomeric states* or *isomers* (or sometimes *metastable* states). There is no clear criterion for classifying a state as isomeric or not; the distinction was originally taken to be whether or not the half-life was directly measurable, but today we can measure half-lives well below 10^{-9} s.

A process that often competes with γ emission is *internal conversion*, in which the nucleus de-excites by transferring its energy directly to an atomic electron, which then appears in the laboratory as a free electron. (This is very different from β decay in that no change of Z or N occurs, although the atom becomes ionized in the process). Studying γ emissions and its competing process, internal conversion, allows us to deduce the spins and parities of the excited states.

Appendix B

Detection Setup of IS441

The detection system consisted of a NE111 plastic scintillator positioned behind the tape at the collection point and used as fast-timing β-detector. The thickness was chosen to have an almost uniform response to the different energies. Two $LaBr_3$:Cs crystals were used as fast-timing gamma detector. In addition, there were two HPGe detectors with energy ranges from 30 to 4000 keV. They were used to provide a unique selection of the γ decay branch in the $\beta-\gamma-\gamma$ method and to study $\gamma-\gamma$ coincidences in order to determine the level scheme. Up to seven parameters were recorded simultaneously for each event, namely the β energy and up to four γ energies plus the time differences between the β signal and a given coincident γ event. The energy and efficiency calibrations of the gamma detectors were determined using sources of ^{140}Ba, ^{138}Cs, ^{152}Eu.

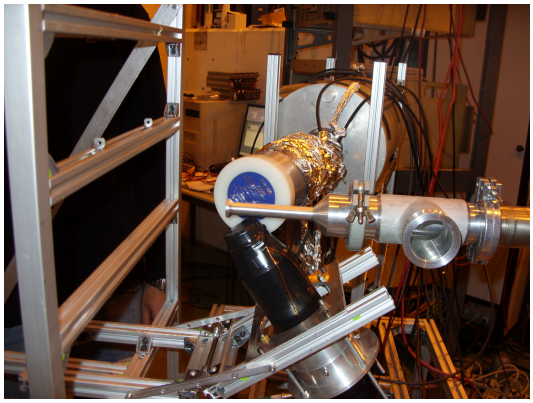

Figure B.1: A picture from the IS441/2011 experiment during the construction of the setup. There are shown one HPGe and one $LaBr_3$:Cs detectors pointing at the spot where the isotopes will be implanted.

Bibliography

[1] Laboratory portrait: The Isolde facility. *Nuclear Physics News International*, 20:5–12, Oct-Dec 2010. (Cited on page 5.)

[2] B. Cheal, J. Billowes, M. L. Bissell, K. Blaum, F. C. Charlwood, K. T. Flanagan, D. H. Forest, S. Fritzsche, Ch. Geppert, A. Jokinen, M. Kowalska, A. Krieger, J. Krämer, E. Mané, I. D. Moore, R. Neugart, G. Neyens, W. Nörtershäuser, M. M. Rajabali, M. Schug, H. H. Stroke, P. Vingerhoets, D. T. Yordanov, and M. Žáková. Discovery of a long-lived low-lying isomeric state in ^{80}Ga. *Phys. Rev. C*, 82:051302, Nov 2010. (Cited on page 3.)

[3] Kenneth S. Krane. *Introductory Nuclear Physics*. John Wiley & Sons, Oregon State University, 1988. (Cited on pages vi and 27.)

[4] XIA LLC. *User's Manual - Digital Gamma Finder (DGF) Pixie-4*. XIA, 31057 Genstar Road Hayward, CA 94544 USA, 2011. (Cited on page 9.)

[5] H. Mach, R.L. Gill, and M. Moszynski. A method for picosecond lifetime measurements for neutron-rich nuclei: (1) outline of the method. *Nuclear Instruments and Methods in Physics Research Section A: Accelerators, Spectrometers, Detectors and Associated Equipment*, 280(1):49 – 72, 1989. (Not cited.)

[6] J. A. Winger, John C. Hill, F. K. Wohn, R. Moreh, R. L. Gill, R. F. Casten, D. D. Warner, A. Piotrowski, and H. Mach. Decay of ^{80}Zn: Implications for shell structure and r -process nucleosynthesis. *Phys. Rev. C*, 36:758–764, Aug 1987. (Cited on page 3.)